Applied Thermal Engineering 29 (2009) 1904–1912

Contents lists available at ScienceDirect

Applied Thermal Engineering

journal homepage: www.elsevier.com/locate/apthermeng

Performance of ejector cooling system with thermal pumping effect using R141b and R365mfc

Jin Hua Wang, J.H. Wu, S.S. Hu, B.J. Huang *

Department of Mechanical Engineering, National Taiwan University, Taipei,Taiwan

ARTICLE INFO

Article history:
Received 30 March 2008
Accepted 20 August 2008
Available online 31 August 2008

Keywords:
Ejector cooling system
Ejector
R365mfc
R141b

ABSTRACT

The ejector cooling system (ECS) is suitable for solar cooling application due to its simple design and low cost. An ECS using a multi-function generator (ECS/MFG) as a thermal pumping device without rotating machines for refrigerant circulation has been designed and tested. The experiment of an ECS/MFG operating at full-cycle while using R141b has shown that the COP_o can reach 0.225 and cooling capacity of 0.75 kW at generator temperature 90 °C, condenser temperature 37 °C, and evaporator temperature 8.5 °C. The present study also redesigned the ejector for working fluid R365mfc in order to replace R141b. This study has shown that R365mfc can replace R141b as the working fluid of ECS/MFG at no pay-off of system performance as long as the ejector design is optimized.

1. Introduction

The ejector cooling system (ECS) is suitable for solar cooling application due to its simple design and low cost. Many researchers were devoted to the study of ejector design to improve the *COP*. Huang et al. [1,2] has shown that the *COP* of an ECS, with a proper design in ejector and system structure, can reach 0.54 at generator temperature 84 °C, condenser temperature 28 °C, and evaporator temperature 8 °C. This makes the ECS may become competitive to the sorption (absorption and adsorption) system that is much more complicated in design and more expensive.

In the ECS, the condenser temperature must be lower than the critical condenser temperature (critical point). Fig. 1 shows the typical performance curve of ECS [1,2]. As the condenser temperature is below the critical point, $T_c < T_c^*$, the ejector performance is under the critical mode and *COP* remains constant. However, when the condenser temperature is increased higher than critical point, $T_c^* < T_c < T_{c0}$, the ejector performance then enters into the sub-critical mode and *COP* decreases with increasing condenser temperature. If the condenser temperature is further increased, $T_c > T_{c0}$, the ejector performance enters into the back-flow mode which is not workable. Therefore, the ejector needs to be operated at critical mode in order to obtain a better performance.

The only rotating machine in the ECS is the mechanical pump for circulating the working fluid from the condenser back to the generator. The mechanical pump is usually inefficient and easy to break down since it operates near the saturated-liquid state. Pump-less technology is thus very important for the commercialization of the ECS.

Nguyen et al. [3] developed a pump-less ECS using a barometric siphon for pumping the working fluid from the low pressure side, condenser, to the high pressure side, generator. This system has minimal maintenance requirement, the potential for a long life time, and a low danger of breakdown. The experimental results show that the system *COP* was 0.32 and cooling capacity was 7 kW at generator temperature 76.7 °C, condenser temperature 26.7 °C, and evaporator temperature 1.5 °C. In this ECS, the condenser has to be raised up to a high enough level, 7 m, to induce a sufficient gravitational force for return of the working fluid back to the generator. This restricts many applications due to the allowable height limit of the machine.

Aphornratana et al. [4] developed a heat-power ECS which employed the workless-generator-feeding (WGF) to replace the mechanical pump. The WGF operated alternately between filling phase and feeding phase. The working fluid was then pumping from condenser to generator via gravity and thermal energy. The prototype using R141b as a working fluid was constructed and tested. The experimental results show that this system was feasible, but it needed more power consumption into the generator to driver the WGF. The generator input power is about 10–15% greater than the ECS using the mechanical pump. Hence, as the WGF operated, it interchanged frequently, the *COP* of this system was comparatively lower.

The ECS can also use a heat-driven pump (HDP) to replace the mechanical pump. Extensive studies related to the HDP were carried out by many researches [5–18]. The HDP requires no rotating machines and no electric power for operation. However, the direct use of HDP in ECS has some problems since the HDP needs some

* Corresponding author. Tel.: +886 2 2363 4790; fax: +886 2 2364 0549.
E-mail address: bjhuang@seed.net.tw (B.J. Huang).

1359-4311/$ - see front matter © 2008 Elsevier Ltd. All rights reserved.
doi:10.1016/j.applthermaleng.2008.08.015

Nomenclature

Symbols

A_r	ejector area ratio, $A_r = (D_t/D_c)^2$
COP	coefficient of performance
C_p	specific heat of water, kJ/kg °C
D_t	nozzle throat diameter, mm
D_c	constant-area diameter, mm
M	mass flow rate of water, kg/sec
P_e	evaporator pressure, MPa
P_{MFGA}	MFG A pressure, MPa
P_{MFGB}	MFG B pressure, MPa
Q_c	total heat output from the condenser, kW
Q_e	cooling capacity, kW
Q_h	total heat input at pressurizing phase, kW
Q_g	total heat input to the generator, kW
T_c	condenser temperature, °C
T_{c0}	condenser temperature of limiting condition, °C
T_c^*	critical condenser temperature, °C
T_e	evaporator temperature, °C
T_{ex}	water exit temperature, °C
T_{in}	water inlet temperature, °C
T_g	generator temperature, °C
W_{mec}	mechanical pump input energy, kW
Δt	operation time of the vapor discharge phase, minute

Subscripts

c	condenser
e	evaporator
g	generator
i	intercooler
max	maximum
set	set point

specially-designed parts to generate mechanical work in order to drive the working fluid. The energy efficiency of the HDP is also very low.

Huang et al. [19] combined the concept of HDP with the design of ECS to come up with the new ejector cooling system without a mechanical pump. The system utilized a multi-function generator (MFG) to eliminate the mechanical pump. This new ECS uses a MFG that acts as a generator for vapor generation and as a feed pump for returning liquid to the generator. The schematic diagram of the ejector cooling system with a multi-function generator (ECS/MFG) is shown in Fig. 2.

There are two MFGs (generators) in the ECS/MFG. Each MFG consists of a vapor generator (boiler) and an evacuation chamber. The vapor generator is a heat exchanger like a conventional boiler for heating the liquid in order to pressurize the whole generator and generate vapor. The evacuation chamber is composed of a cooling jacket and a liquid tank. The cooling jacket provides a cooling effect to depressurize the whole generator in order to intake the liquid from the condenser.

The two MFGs (MFG A and B) operate interchangeably through the control switching valves and check valves. The operation of each MFG can be divided into four phases: pressurizing, vapor discharge, depressurizing, and liquid intake. While MFG A is operating at depressurizing, liquid intake, and pressurizing phases, MFG B is operating at the vapor discharge phase. The cooling effect of the ECS/MFG is generated only at the vapor discharge phase. So, the design of a MFG thus requires the total time duration for depressurizing, liquid intake and pressurizing phases shorter than the period of discharge phase. The processes of the pressure variation of two MFGs are shown in Fig. 3.

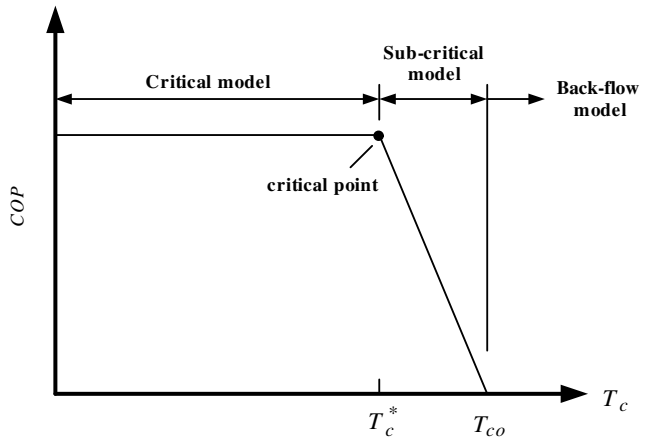

Fig. 1. Performance curve of ECS.

Huang et al. [19] built a prototype of the ECS/MFG using only one MFG (generator) for studying the feasibility of the new design concept. This machine is similar to absorption cooling system with half effect working model. The measured COP_o for the half-cycle run with R141b was 0.218 and the cooling capacity was 0.786 kW at generator temperature 90 °C, condenser temperature 32.4 °C, and evaporator temperature 8.2 °C. It was shown that a continuous operation for the generation of cooling effect in the ECS/MFG could be achieved.

According to the working principle, one MFG can only produce a half-cycle cooling effect. Therefore, two MFGs need to be coupled together to generate a continuous cooling effect which is namely full cycle operation. The switching valves would be suitably manipulated to synchronize between the two MFGs. The present study continues this research to develop a proper switching technique for the ECS/MFG to run in full cycle and carry out the performance test in full cycle.

Although the refrigerant R141b used in the experiment although has good performance, it still needs to be replaced with a low ODP working fluid. This requires modification of the ejector design in order to maintain a high *COP*. The R365mfc with zero ODP is a relatively new working fluid and has never been tested in the ECS. Bobbo et al. [20] described some its thermodynamic behavior. Table 1 lists some relevant properties of R141b and R365mfc. The present study also investigates the design of the ejector using R365mfc, in order to obtain a good performance of ECS/MFG.

2. Design of ejector cooling system with multi-function generator (ECS/MFG)

The prototype design of the ECS/MFG is basically the same as those described in [19], but with an automatic controller and two MFGs to obtain a full-cycle continuous operation as shown in Fig. 4.

Table 2 shows the design of the ejectors used in the experiments. For refrigerant R141b, the ejector area ratio, $A_r = (D_t/D_c)^2$, is 7.73 which gives a good performance according to the previous study [1,2]. The nozzle and constant-area sections were selected for the ejector operated at critical-model. For R365mfc, the ejector needs to be magnified since its latent heat is lower than R141b (Ta-

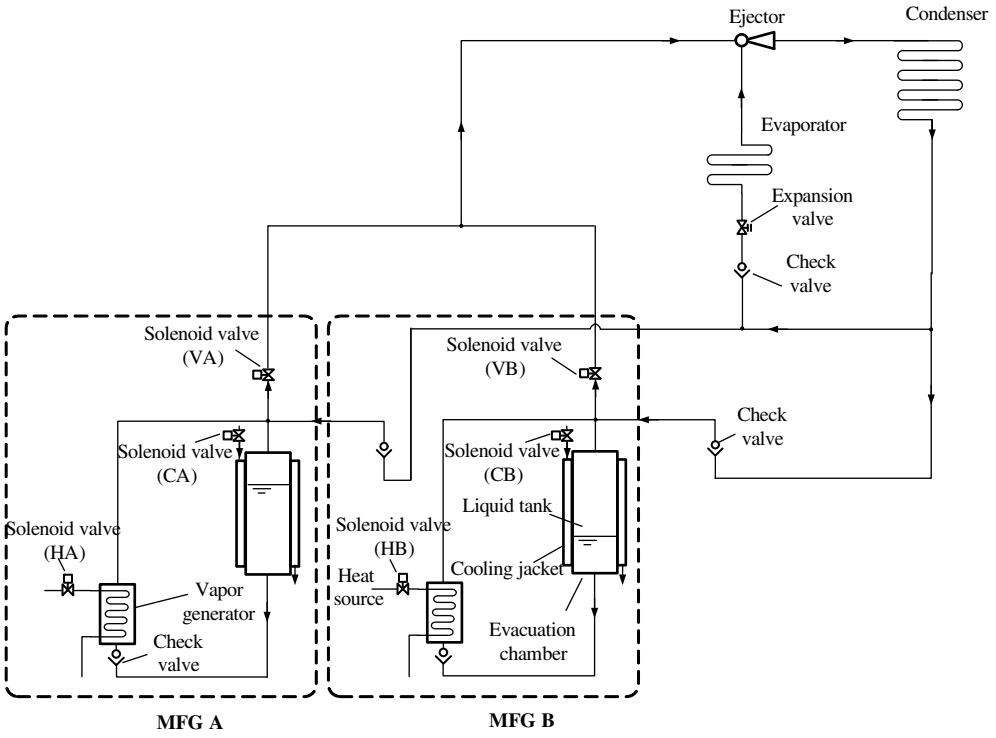

Fig. 2. Flow diagram of ejector cooling system with multi-function generator (ECS/MFG).

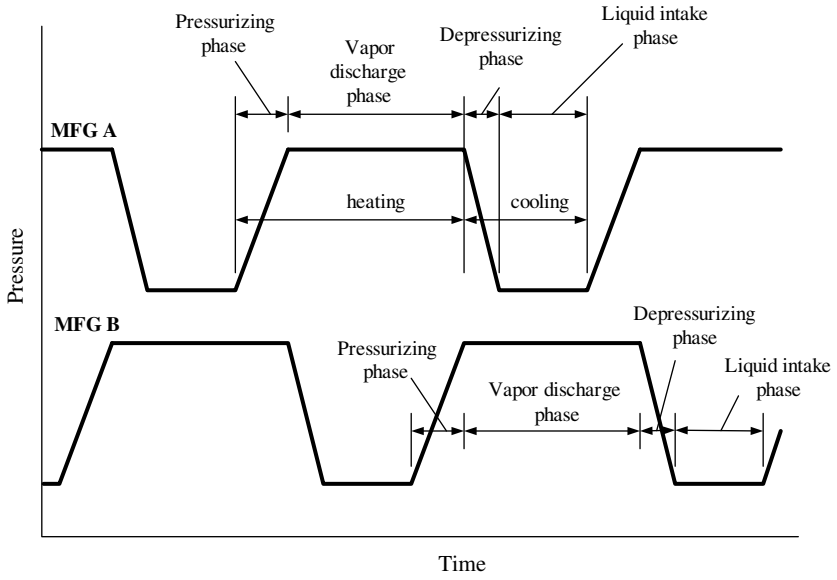

Fig. 3. Pressure variation of two MFGs.

Table 1
Thermodynamic property of R141b and R365mfc

Working fluid	Formula	Molecular weight	Normal boiling point temperature at 1atm (°C)	Latent heat at 1 atm(kJ/kg)	ODP relative to R11
R141b	CH_3CCl_2F	117	32	222.7	0.11
R365mfc	$CF_3CH_2CF_2CH_3$	148	40	192.8	0

ble 1). Hence, we designed another ejector with area ratio of 9.10 and 11.03 to compare the performance.

The automatic controller was utilized to obtain a full-cycle continuous operation and a constant evaporator temperature. The two MFGs operate interchangeably between pressurizing, vapor discharge, depressurizing, and liquid intake phases by an automatic controller to control the six solenoid valves (VA, VB, HA, HB, CA and CB) according to the algorithm shown in Table 3.

The automatic controller of ECS/MFG needs to measure evaporator pressure (P_e), two MFG pressures (P_{MFGA} and P_{MFGB}), and the operating time of the vapor discharge phase (Δt_{MFGA} and Δt_{MFGB}). Fig. 5 shows sequence diagram of the ECS/MFG. As the MFG A is at the pressurizing phase, the vapor generator is heated with only the HA opened. At this time, the MFG B is operating at

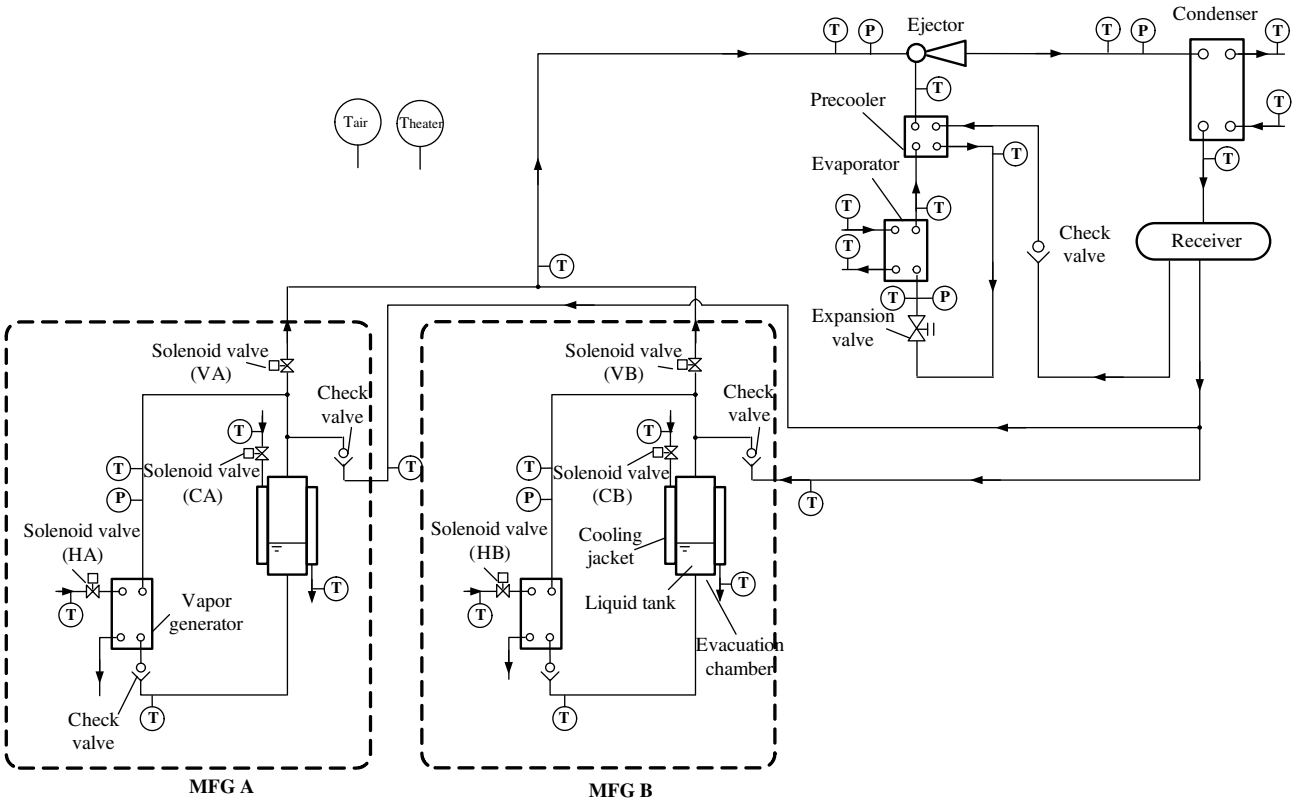

Fig. 4. Schematic description of experimental setup.

Table 2
Design of nozzle and constant-area section

Nozzle		Constant-area section		Ejector specification
Throat diameter (mm)	Exit diameter (mm)	Constant-area diameter (mm)	Inlet converging angle (°)	Ejector area ratio
2.64	4.50	7.34	60	7.73
2.93	4.46	8.84	67	9.10
2.80	5.10	9.30	65	11.03

Table 3
Working states of two MFGs (O: open; X: close)

MFG_A	Pressurizing phase	Vapor discharge phase	Vapor discharge phase	Depressurizing phase and liquid intake phase
MFG_B	Vapor discharge phase	Depressurizing phase and liquid intake phase	Pressurizing phase	Vapor discharge phase
HA	O	O	O	X
VA	X	O	O	X
CA	X	X	X	O
HB	O	X	O	O
VB	O	X	X	O
CB	X	O	X	X

a vapor discharge phase with the VB and HB opened. In the vapor discharge phase of either MFGs, the cooling effect of the ECS/MFG is generated. The vapor discharge phase of the MFG B is terminated when the evaporator pressure is higher than the set point (P_{e_set}) at 0.004 MPa, at which the cooling effect will be unstable.

MFG B enters into the depressurizing phase with the CB opened, the HB and VB closed to cool down the evacuation chamber. At this moment, the pressure in the MFG A rises to a level that can drive the ejector. MFG A then enters into the vapor discharge phase with the VA opened. The vapor is discharged to activate the ejector to produce a cooling effect. As the MFG B pressure is lower than the condenser, the check valve is opened to induce the liquid refrigerant return from the condenser. The MFG B enters into the liquid intake phase with the evacuation chamber still being cooled. In the initial three minutes when the MFG A enters into the vapor discharge phase, the MFG A pressure has some fluctuation since the system is not steady yet. In the vapor discharge phase, the MFG pressure has a maximum value. Once the MFG A pressure is lower than the maximum value at 0.004 MPa, the MFG A is nearly empty and the MFG B then enters into the pressurizing phase with the CB closed and the HB opened. Another switch condition is the operating time of the vapor discharge phase for about six minutes which is related the volume of the liquid tank. As the evaporator pressure is higher than the set point 0.004 MPa, the MFG A and MFG B are interchanged again. According to the sequence diagram, the ECS/MFG can operate sequentially and produce a stably cooling effect.

The system was installed with twenty-six T-type thermocouples with an uncertainty of ± 0.7 °C, and five pressure transducers within a ±1% uncertainty (see Fig. 4). Thermocouples and transducers were installed at different locations [19]. The power consumption of the electrical heater was measured by a power meter within a ±1.5% uncertainty. The water flow rate of the evaporator, condenser, and cooling of the MFG were measured using water flow meters within a ±4% uncertainty.

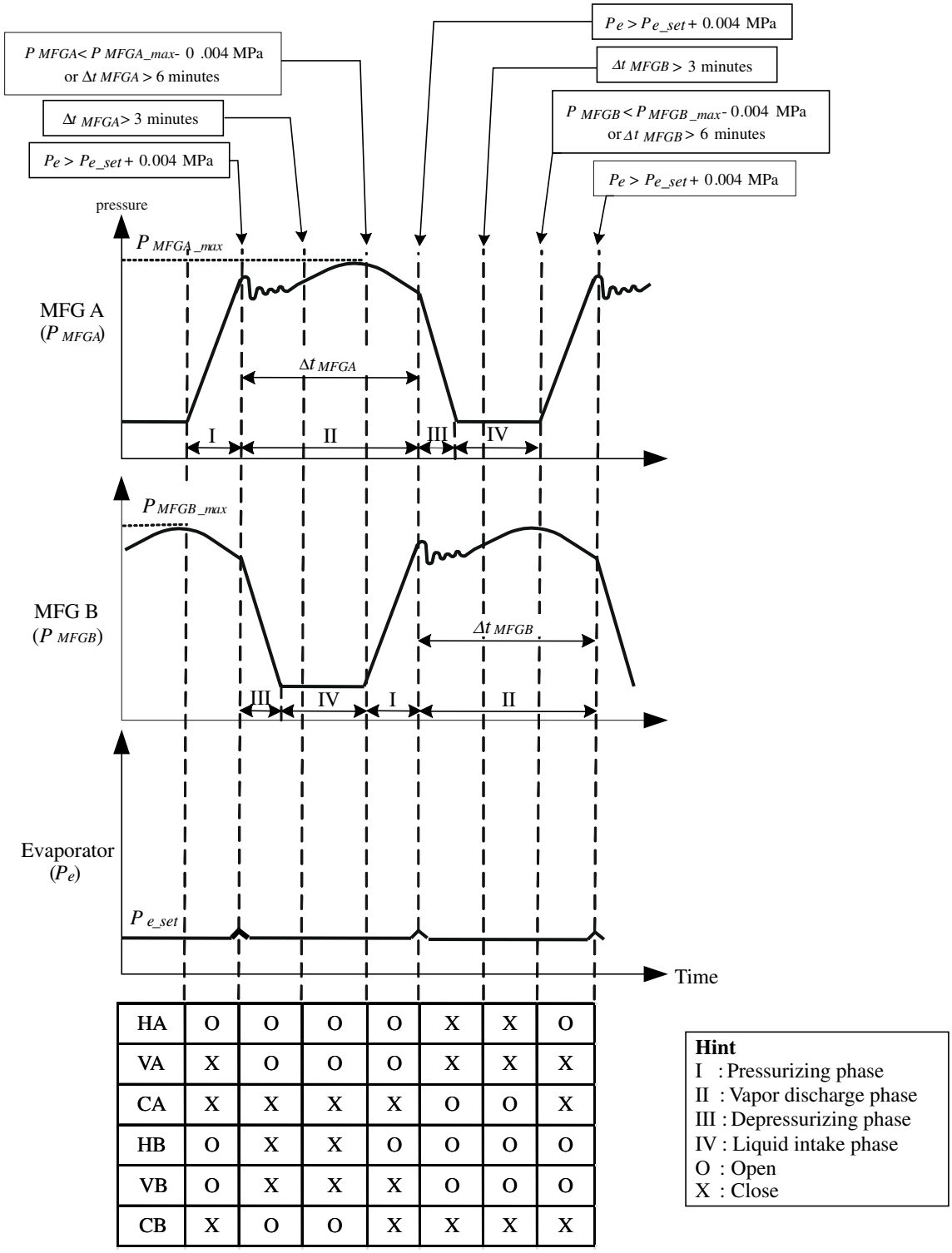

Fig. 5. Sequence diagram of automatic controller.

3. Experimental results and discussion

3.1. Continuous full-cycle operation of ECS/MFG using R141b

The *COP* of an ejector cooling system is defined as

$$COP = \frac{Q_e}{Q_g + W_{mec}} \quad (1)$$

The pumping power, W_{mec}, is neglected here since the system utilizes a multi-function generator (MFG) to eliminate the mechanical pump. Therefore, the *COP* of the ECS/MFG is defined as the ratio of the cooling capacity at the evaporator, Q_e, to the total heat input to the generator (MFG), Q_g. Two *COP*s are further defined and determined [19]. The system *COP* at vapor discharge phase, COP_o, is defined as:

$$COP_o = \frac{\text{Total cooling energy obtained at vapor discharge phase}}{\text{Total heat input at vapor discharge phase}} = \frac{Q_e}{Q_g} = \frac{Q_e}{Q_c - Q_e} \quad (2)$$

The cooling capacity, Q_e, and total heat output from the condenser, Q_c, are determined by an energy balance using the water flow rate and water temperature difference between the inlet and outlet.

$$Q_e = M_e C_p (T_{ex} - T_{in})_e \quad (3)$$

$$Q_c = M_c C_p (T_{ex} - T_{in})_c \quad (4)$$

COP_t is another COP taking into account the extra heat needed for liquid pumping process in the MFG. The total system COP, COP_t, is defined as:

$$COP_t = \frac{\text{Total cooling energy obtained at vapor discharge phase}}{\text{Total heat input per cycle}} = \frac{Q_e}{Q_h + Q_g} = \frac{Q_e}{Q_h + Q_c - Q_e} \quad (5)$$

The main objective of this experiment was to study the continuous full-cycle operation of the ECS/MFG. The ECS/MFG was tested by R141b and ejector area ratio of 7.73 at an ambient temperature around 25 °C. A preliminary test for adjusting a suitable amount of filling refrigerant was done first. The experimental result is shown in Fig. 6. Each temperature line was converted from pressure measurement using R141b thermodynamic chart. The ECS/MFG can be manipulated to synchronize between the two MFGs. While MFG A was operating at the depressurizing phase, liquid intake phase, and pressurizing phase, MFG B was operating at the vapor discharge phase. The total time period of depressurizing, liquid intake, and pressurizing phase is less than the vapor discharge time. The experimental results show that the ECS/MFG can produce continuous cooling effect. The generator temperature, condenser temperature, and evaporator temperature remained almost constant. The

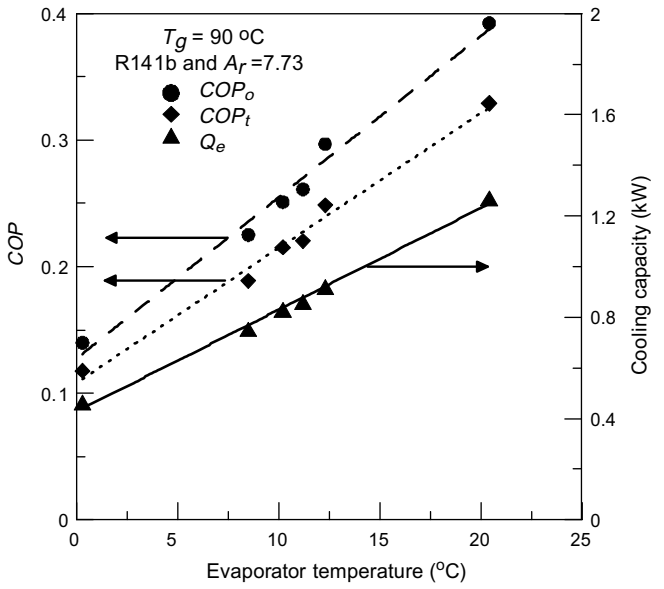

Fig. 7. *COP* and cooling capacity of ECS/MFG using R141b and ejector area ratio with 7.73.

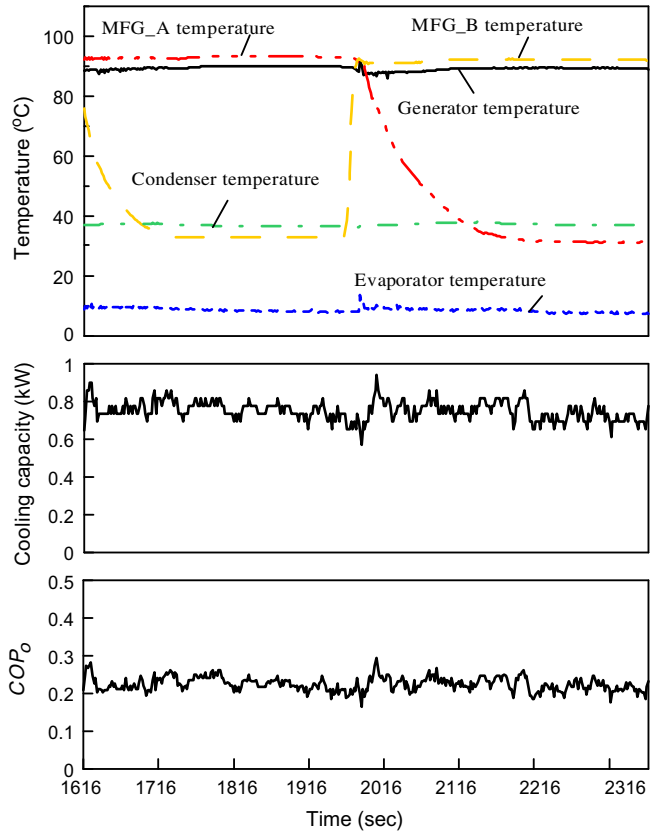

Fig. 6. Continuous full-cycle operation of ECS/MFG using R141b and ejector area ratio with 7.73.

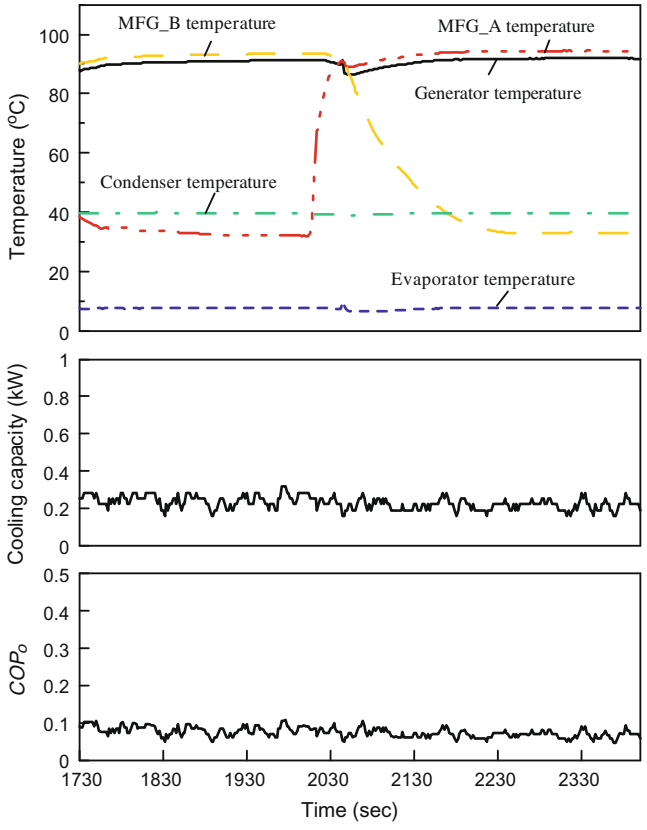

Fig. 8. Continuous full-cycle operation of ECS/MFG using R365mfc and ejector area ratio with 7.73.

average COP_o is 0.225 and cooling capacity is 0.75 kW at average generator temperature 89.1 °C, condenser temperature 37.0 °C, and evaporator temperature 8.5 °C.

A variation of the COP_t and cooling capacity with evaporator temperature at generator temperature around 90 °C are shown in Fig. 7. The COP_o changes from 0.140 to 0.392, COP_t changes from 0.118 to 0.329, and the cooling capacity changes from 0.46 kW to 1.27 kW, when the evaporator temperatures are varied between 0.3 and 20.4 °C. Both *COP* and cooling capacity increase almost linearly with the evaporator temperature.

3.2. Continuous full-cycle operation of ECS/MFG using R365mfc

The ejector of the ECS/MFG system uses the same ejector with area ratio (A_r = 7.73) to run with the R365mfc to study the feasibility of continuous operation and system performance. The experimental result is shown in Fig. 8. Similarly, each temperature line was converted from pressure measurement. Fig. 8 indicates that the system can continuously operate in full-cycle but with poor performance. The average COP_o is 0.074 and cooling capacity is 0.23 kW at generator temperature 90.8 °C, condenser temperature 39.6 °C, and evaporator temperature 7.6 °C. Variation of COP_o, COP_t, and cooling capacity with evaporator temperature at generator temperature around 90 °C are shown in Fig. 9. The trends in *COP* and cooling capacity variation with evaporator temperature are similar to those of Fig. 7. However, the COP_o, COP_t, and cooling capacity are much lower than that of the experiment using R141b (Fig. 7). The ejector design needs to be optimized for the R365mfc.

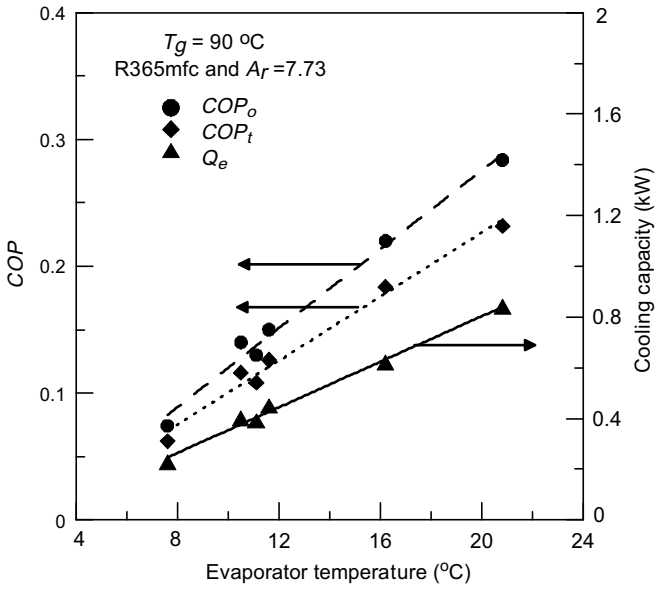

Fig. 9. *COP* and cooling capacity of ECS/MFG using R365mfc and ejector area ratio with 7.73.

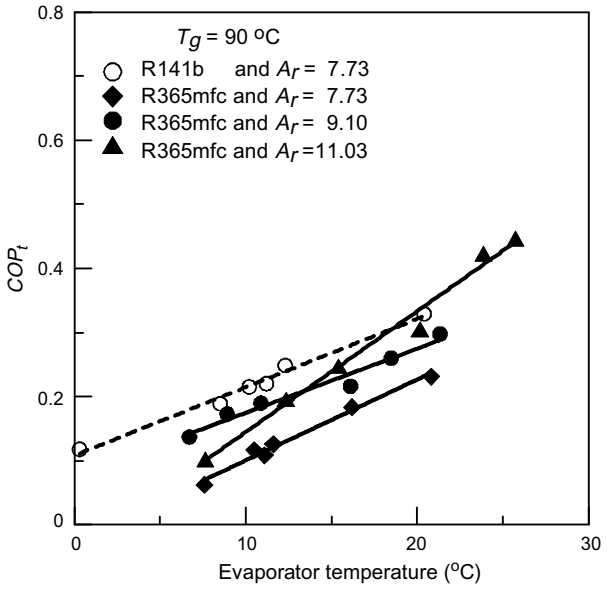

Fig. 11. COP_t for different ejector designs.

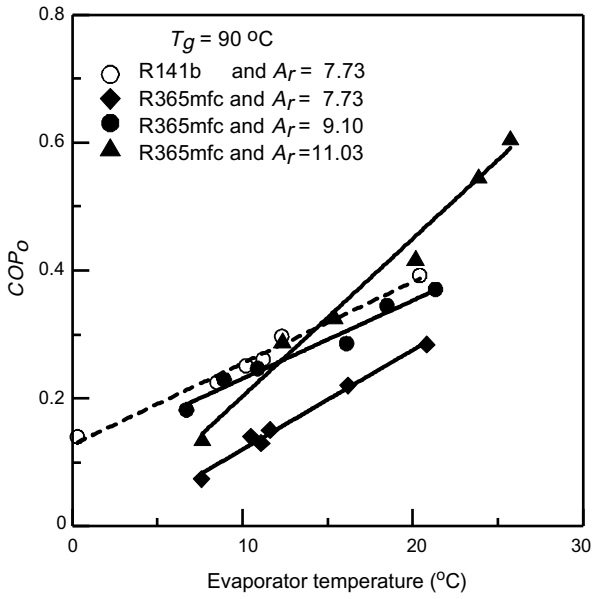

Fig. 10. COP_o for different ejector designs.

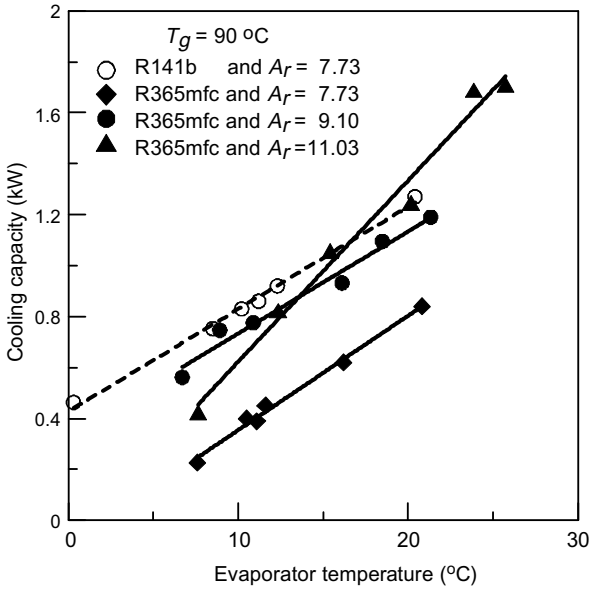

Fig. 12. Cooling capacity curves for four different operation conditions.

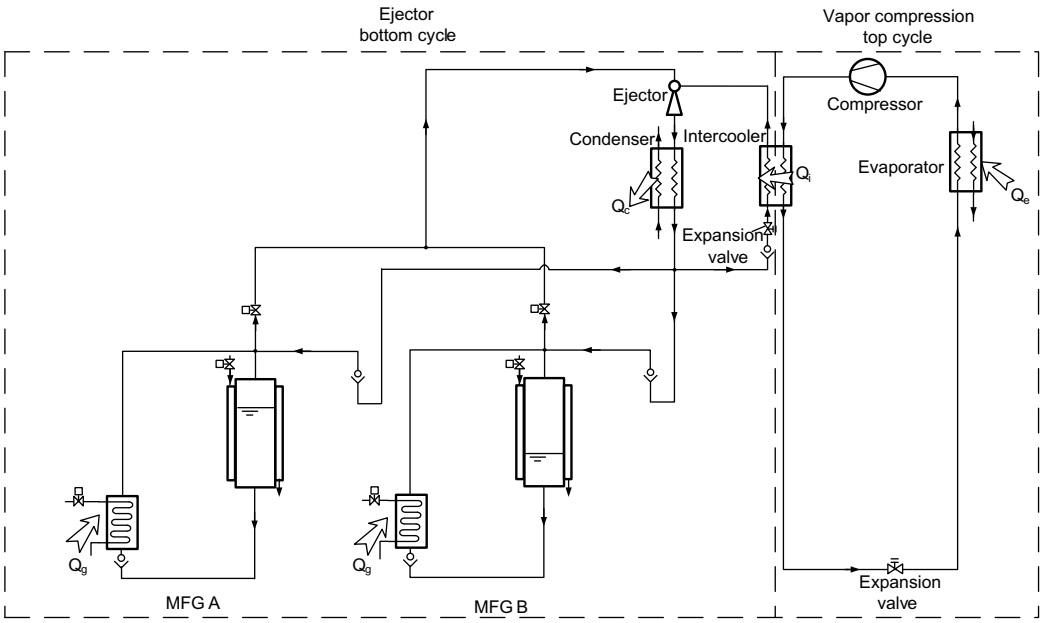

Fig. 13. Schematic of solar-powered ejector air conditioner.

The ECS/MFG used ejector area ratio of 9.10 and 11.03 for replacing the original ejector ($A_r = 7.73$). Figs. 10–12 show the COP_o, COP_t, and cooling capacity curves for different operation conditions at the generator temperature 90 °C, respectively. For an ejector with ejector area ratio of 9.10 to run with R365mfc, the system performance is improved significantly. At generator temperature 90 °C, COP_o varies from 0.182 to 0.371, COP_t varies from 0.137 to 0.298, and cooling capacity varies from 0.56 kW to 1.20 kW for evaporator temperatures varied between 6.7 and 21.3 °C. As can be seen from the ejector area ratio of 7.73 for R141b and ejector area ratio of 9.10 for R365mfc, COP_o, COP_t and cooling capacity are nearly identical with each other at the same operating conditions. This result has shown that R365mfc can replace R141b at no payoff of system performance, as long as the ejector design is optimized.

For an ejector with ejector area ratio of 11.03 to run with R365mfc, COP_o varies from 0.137 to 0.608, COP_t varies from 0.102 to 0.446, and cooling capacity varies from 0.42 kW to 1.71 kW, for evaporator temperatures varied between 7.6 and 25.7 °C at generator temperature 90 °C.

4. Discussions and conclusion

The ejector cooling system (ECS) is suitable for solar cooling application due to its simple design and low cost. In the present study, the ejector cooling system using a multi-function generator (ECS/MFG) as a thermal pumping was constructed and tested. Some important results are obtained as follows:

(1) The experimental result has shown that the ECS/MFG can operate continuously at full cycle by a switching control of the two MFGs. This system can be very reliable since there is no circulation pump.
(2) The ECS/MFG operating at full-cycle and using R141b as the refrigerant can achieve a COP_o of 0.225 and cooling capacity of 0.75 kW at generator temperature 90 °C, condenser temperature 37 °C and evaporator temperature 8.5 °C. The experimental results are similar to the half-cycle of Huang et al. [19] under the same operating conditions.
(3) The present study also redesigned the ejector for working fluid R365mfc in order to replace R141b which was phased out. We have shown experimentally that R365mfc can replace R141b at no payoff of system performance as long as the ejector design is optimized.
(4) In the solar-powered ejector air conditioner [21–26], the ejector cooling cycle and vapor compression cycle would be combined together as shown in Fig. 13. The common component of the two cycles was the intercooler which was a heat exchanger. In this case, the ejector bottom cycle needed to operate at higher evaporator temperatures. Sokolove et al. [21–23] had shown that the evaporator temperature was about 31 °C. The ECS/MFG which used R365mfc as a working fluid with ejector area ratio of 11.03 can be operated at evaporator temperature 25.7 °C with COP_o up to 0.608 and COP_t up to 0.446. It is more suitable for solar-powered ejector air conditioner.

Acknowledgement

The present study was supported by Energy Bureau, Ministry of Economic Affairs, Taiwan.

References

[1] B.J. Huang, J.M. Chang, Empirical correlation for ejector design, Int. J. Refrigeration 22 (1999) 379–388.
[2] B.J. Huang, J.M. Chang, C.P. Wang, V.A. Petrenko, A 1D analysis of ejector performance, Int. J. Refrigeration 22 (1999) 354–364.
[3] V.M. Nguyen, S.B. Riffat, P.S. Doherty, Development of a solar-powered passive ejector cooling system, Appl. Therm. Eng. 21 (2001) 157–168.
[4] P. Srisastra, S. Aphornratana, T. Sriveerakul, Development of a circulating system for a jet refrigeration cycle, Int. J. Refrigeration (2007).
[5] Y.W. Wong, K. Sumathy, Solar thermal water pumping systems: a review, Renewable Sustainable Energy Rev. 3 (1999) 185–217.
[6] D.P. Rao, K.S. Rao, Solar water pump for lift irrigation, Solar Energy 18 (1976) 405–411.
[7] K. Sudhakar, M. Murali Krishna, D.P. Rao, Analysis and simulation of a solar water pump for lift irrigation, Solar Energy 24 (1979) 71–82.
[8] M.P. Sharma, G. Singh, A low lift solar water pump, Solar Energy 25 (1980) 273–278.
[9] R. Burton, A solar powered diaphragm pump, Solar Energy 31 (1983) 523–525.

[10] K. Sumathy, A. Venkatesh, V. Sriramulu, Thermodynamic analysis of a solar thermal water pump, Solar Energy 57 (1996) 155–161.
[11] A.A. Al-Haddad, E. Enaya, M.A. Fahim, Performance of modynamic water pump, Appl. Therm. Eng. 16 (1996) 321–334.
[12] K. Sumathy, Experimental studies on a solar thermal water pump, Appl. Therm. Eng. 19 (1999) 449–459.
[13] V.J. Sasin, L.X. Hoa, N.M. Savchenkova, N.T.B. Ngoc, Outlook at application of bi-phase pulsing contour with intermediate vessel, IV Minsk international seminar 'heat pipes, heat pumps, refrigerators' (2000) 42–49.
[14] Y.W. Wong, K. Sumathy, Thermodynamic analysis and optimization of a solar thermal water pump, Appl. Thermal Eng. 21 (2001) 613–627.
[15] V.J. Sasin, L.X. Hoa, N.M. Savchenkova, Outlook at application of bi-phase pulsing contour for heat supply and cooling systems, in: Proceedings of the Twelth International Heat Pipe Conference, Russia (2002) 448–453.
[16] J.L. Xu, X.Y. Huang, T.N. Wong, Study on heat driven pump. Part 1—experimental measurements, Int. J. Heat Mass Transfer 46 (2003) 3329–3335.
[17] J.L. Xu, T.N. Wong, X.Y. Huang, Study on heat driven pump. Part 2—mathematical modeling, Int. J. Heat Mass Transfer 46 (2003) 3337–3347.
[18] D. Das, M. Ram Gopal, Studies on a metal hydride based solar water pump, Int. J. Hydrogen Energy 29 (2004) 103–112.
[19] B.J. Huang, S.S. Hu, S.H. Lee, Development of an ejector cooling system with thermal pumping effect, Int. J. Refrigeration 29 (2006) 476–484.
[20] S. Boobo, M. Scattolini, L. Fedele, R. Camporese, Compressed liquid densities and saturated liquid densities of HFC-365mfc, Fluid Phase Equilibr. 222-223 (2004) 291–296.
[21] M. Sokolov, D. Hershgal, Enhanced ejector refrigeration cycles powered by low grade heat. Part 1. systems characterization, Int. J. Refrigeration 13 (1990) 351–356.
[22] M. Sokolov, D. Hershgal, Enhanced ejector refrigeration cycles powered by low grade heat. Part 2 design procedures, Int. J. Refrigeration 13 (1990) 357–363.
[23] M. Sokolov, D. Hershgal, Enhanced ejector refrigeration cycles powered by low grade heat. Part 3 experimental results, Int. J. Refrigeration 14 (1991) 24–31.
[24] A. Arbel, M. Sokolov, Revisiting solar-powered ejector air conditioner the greener the better, Solar Energy 77 (2004) 57–66.
[25] J.I. Hernández, R.J. Dorantes, R. Best, C.A. Estrada, The behaviour of a hybrid compressor and ejector refrigeration system with refrigerants 134a and 142b, Appl. Therm. Eng. 24 (2004) 1765–1783.
[26] D.W. Sun, Solar powered combined ejector-vapour compression cycle for air conditioning and refrigeration, Energy Conver Manage 38 (1997) 479–491.